JOURNAL OF SPACECRAFT AND ROCKETS
Vol. 37, No. 2, March–April 2000

Attitude Control System Design for Return of the Kistler K1 Orbital Vehicle

David S. Rubenstein* and David W. Carter†
Charles Stark Draper Laboratory, Inc., Cambridge, Massachusetts 02139

An attitude control system design is presented that provides the maneuver capability and aerodynamic angle maintenance necessary for the atmospheric reentry and return to launch site of an unmanned reusable launch vehicle. The primary functions are categorized into those that perform bank maneuvers about the air-relative velocity vector and those that are responsible for the tracking and control of the vehicle aerodynamic trim conditions. The control system is supported by an onboard aerodynamic estimation function. The estimator uses measurements of vehicle states from navigation in combination with analytic models in a gain-scheduled filter environment to provide control with current trim angle information. The control system uses this information to minimize actual vehicle deviations from the trim. Also, control is provided with bank commands from a guidance function. As this paper is concerned only with the control and estimation functions, the guidance strategies are discussed only to the extent that is necessary to justify/clarify control or estimator designs. The algorithms developed here are applied to the Kistler K1 Orbital Vehicle and tested in the Kistler Integrated Vehicle Simulation at Draper Laboratory. Results indicate that the approach to entry/return control is both fuel efficient and effective from a landing accuracy perspective.

Nomenclature

A = characteristic amplitude of angle-of-attack oscillations, rad
a_I = inertial acceleration of vehicle expressed in inertial frame, ft/s^2
C_A, C_N = axial and normal aerodynamic force coefficients
$C_{A,\alpha}$, $C_{N,\alpha}$ = partial derivatives of axial and normal aerodynamic force coefficients with respect to angle of attack, 1/rad
F_{aero} = estimated aerodynamic force vector in the inertial frame, lb
F_{ENTRY} = axial force threshold for determining if in atmosphere, lb
F_{jets} = control jet force vector in body frame, lb
h = altitude above sea-level, ft
I_{xx}, I_{yy}, I_{zz} = principal moments of inertia in body frame, slug-ft^2
$\boldsymbol{J}$ = vector of selected attitude control system jets required to bring about the computed attitude control
K_β, $K_{\dot\beta}$ = gains on sideslip correction vectors
K_θ = gain used in the determination of acceptable maximum bank maneuver rate
K_ϕ = gain used in computation of attitude error to prioritize components
$K_{\dot\phi}$ = gain used in computation of attitude rate error to prioritize components
L = gain vector for trim estimator
M = Mach number
N_{jets} = control jet torque vector in body frame, ft-lb
Q = dynamic pressure ($\frac{1}{2}\rho\|v_{\text{air}}\|^2$), lb/ft^2
q_{IB} = current inertial-to-body attitude quaternion
R_{CMD} = rotation command vector output from control
r_I = current inertial position vector in inertial frame, ft
${}_B T_I$ = direction cosine matrix transforming from inertial to body coordinates
v_{air} = current velocity relative to atmosphere in body frame, ft/s
v_I = current inertial velocity vector in inertial frame, ft/s
v_{sound} = speed of sound, ft/s
v_{targ} = desired or target rotation axis for bank maneuvers, ft/s
x_{cp} = longitudinal coordinate of the aerodynamic center of pressure, ft
x_{cg}, z_{cg} = x and z axes location of c.g. in body reference, ft
α, α^*, β = aerodynamic angle of attack, total angle of attack, and sideslip from navigation measurements, rad
α_{trim}, β_{trim} = estimated values of aerodynamic trim angles, rad
$\boldsymbol{\beta}$, $\dot{\boldsymbol{\beta}}$ = desired sideslip and sideslip rate correction vectors, rad, rad/s
Δt_p = time since last pitch control firing in bank coupling control, s
$\Delta\phi$ = required angular change for bank control, rad
$\boldsymbol{\theta}$ = actual amount of rotation remaining in a maneuver, rad
$\ddot{\theta}_{CC}$ = Euler coupling acceleration vector, rad/s^2
θ_d = target remaining rotation angle for a given maneuver, rad
$\ddot{\theta}_{\text{man}}$ = nominal anticipated control acceleration vector, rad/s^2
$\dot{\theta}_V$ = vector of inertial angular rate of velocity vector expressed in body frame, rad/s
$\dot{\theta}_{\text{VCR}}$ = vector of inertial angular rate of bank ($v_I \times r_I$) vector expressed in body frame, rad/s
θ_1, θ_2, θ_3 = target angles of three segments of bank maneuver, representing both roll and yaw axes portions, rad
$\dot{\theta}_1$, $\dot{\theta}_2$, $\dot{\theta}_3$ = target rate of three segments of bank maneuver, representing both roll and yaw axes portions, rad/s
$\ddot{\theta}_1$, $\ddot{\theta}_2$, $\ddot{\theta}_3$ = target acceleration of three segments of bank maneuver, representing both roll and yaw axes portions, rad/s^2
ρ = atmospheric density, lbm/ft^3
$\boldsymbol{\phi}$ = desired bank maneuver rotation vector, rad

Received 25 October 1998; revision received 20 November 1999; accepted for publication 8 December 1999. Copyright © 2000 by the American Institute of Aeronautics and Astronautics, Inc. All rights reserved.

*Senior Member of the Technical Staff, MS 77, 555 Technology Square. Senior Member AIAA.
†Principal Member of the Technical Staff, MS 77, 555 Technology Square.

ϕ_{current} = current aerodynamic bank angle, rad
ϕ_{NC} = current commanded vehicle bank angle from guidance function, rad
$\dot{\phi}_{\text{NC}}$ = current commanded vehicle bank angle rate from guidance function, rad
ϕ_{OC} = previous commanded vehicle bank angle from guidance function, rad
Ω = characteristic frequency of angle-of-attack oscillations, rad/s
$\omega(\omega_x, \omega_y, \omega_z)$ = inertial angular rate vector of vehicle expressed in body fixed frame, rad/s
ω_{old} = initial angular rate vector for construction of a bank maneuver, rad/s

Introduction

THE Kistler K1 vehicle is an unmanned reusable launch system that is intended to deliver payloads to low Earth orbit and return to Earth, landing within a designated target radius and in a condition conducive to rapid turnaround for reuse up to 100 times with a minimum of maintenance and preparation. A diagram depicting the basic mission profile is shown in Fig. 1. The vehicle consists of two stages: the first stage is launch assist platform (LAP), and the second stage is orbital vehicle (OV). The LAP lifts the combined stack to an altitude from which the OV can achieve the necessary orbital conditions and then returns to the landing site, landing with parachutes and airbags. After achieving orbit and deploying the payload, the OV reenters the atmosphere and, using active guidance and control, negotiates the required maneuvers to attain a trajectory that will result in a safe and accurate return to the landing site, also landing with parachutes and airbags. The attitude control system responds to commands from the guidance system by constructing and executing bank maneuvers to rotate the lift vector strategically. Additionally, the control system must monitor and maintain various aerodynamic conditions (such as α and β) associated with performing effective and efficient banks. This work presents the approach to bank maneuver construction, aerodynamic parameter maintenance and estimation philosophies and design, and application of the phase-plane control concept to the atmospheric reentry problem. The Kistler flight software is categorized into three primary functions: guidance, navigation, and control. The subject of this work is the design and implementation of the control system only. The paper is not concerned with the details of the onboard guidance or navigation functions. They are discussed only as needed to depict clearly the function of the control system, in terms of inputs, outputs, and responsibilities.

Attitude Control System Design

The K1 OV attitude control system is responsible for controlling the vehicle from shortly after the de-orbit burn through atmospheric reentry and landing under the OV main parachute system. The control system consists of three main modes of operation to accommodate the unique requirements for the different mission phases. The entry control (EC) mode is the primary mode of operation and is active from just beyond deorbit (when hand-over from the OV on-orbit control system occurs) through atmospheric reentry. The EC mode is terminated upon deployment of the OV stabilization parachute. This action is triggered by a Mach-number threshold (likely in the vicinity of 2.6). The primary role of the EC mode is the intelligent construction and execution of coordinated bank-about-velocity commands from the OV entry guidance system required to return the vehicle safely to the target landing zone.

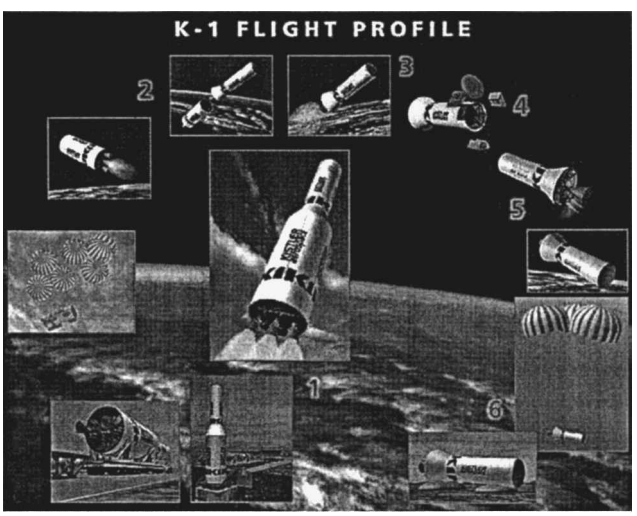

Fig. 1 K1 OV mission profile [source: Kistler Aerospace Corporation Web site (http://www.kistleraerospace.com/fp/home.html)].

Additionally, during EC, the control system will monitor and maintain critical aerodynamic parameters necessary for efficient and effective banks. An aerodynamic estimator, which estimates the current trim conditions for the OV, provides EC with additional information necessary to maintain precisely the desired lifting characteristics on the vehicle.

The other modes in which the controller operates are the yaw-to-velocity (YC) mode responsible for reorienting the OV while under the main parachute system such that the vehicle longitudinal axis is aligned with the Earth relative velocity direction and the monitor-for-yaw (MC) mode, which simply monitors vehicle states to determine if it is time to transition to the YC mode. The MC mode produces no attitude control commands. The YC mode is intended to ensure that the OV can land safely on the landing airbag system.

This paper is concerned only with the EC mode of the controller. It describes the basic technical approach for the EC maneuver construction and control as well as the approach to aerodynamic estimation. Flow diagrams and figures are used to clarify design and implementation. The EC mode constructs and executes the desired bank-about-velocity maneuvers and monitors and maintains the necessary aerodynamic conditions. To accomplish these tasks, EC must perform several critical activities as follows and as depicted in Fig. 2:

1) Compute current actual aerodynamic bank, sideslip, and angle of attack (ϕ, β, α).

2) Perform aerodynamic estimation to provide information needed for efficient control. These include the current trim angle of attack α_{trim}, the characteristic frequency of the angle-of-attack oscillations Ω, and the amplitude of these oscillations A.

3) Compute the current Euler coupling accelerations $\ddot{\theta}_{CC}$.

4) Determine the correct (signed) delta-bank $\Delta\phi$ maneuver necessary to accomplish the guidance command.

5) Compute the rotational rates of the air-relative velocity vector and the bank vector.

6) Construct the appropriate rotation vector for the bank maneuver.

7) Determine necessary correction for sideslip maintenance.

8) Compute the current angle and rate errors (discussed in Computation of Angle and Rate Errors section) associated with the current vehicle state. (For banks/sideslip control this will include only the roll and yaw axes.)

9) Determine the appropriate control action for the bank, based on these errors, using a phase-plane control implementation.

10) Determine the appropriate pitch-axis command based on information from the estimator and the vehicle state.

11) Generate the necessary attitude control system (ACS) jet selection vector from a simple look-up table, based on the desired control actions.

The EC controller requires various inputs from several sources. In particular, the OV navigation function provides the controller with the 1) current position vector in the inertial reference frame r_I, 2) current inertial velocity in the inertial frame v_I, 3) current inertial-to-body attitude quaternion q_{IB}, and 4) current inertial angular rate in the OV body frame ω.

The OV guidance function provides the controller with the 1) current vehicle commanded aerodynamic bank angle ϕ_{NC} and 2) the current vehicle commanded bank rate $\dot{\phi}_{\text{NC}}$.

The OV EC initialization function provides the controller with the 1) jet force and torque vector from the previous cycle F_{jets}, N_{jets} and 2) the current aerodynamic force in the inertial frame (this is estimated using measurements of integrated specific force compensated for ACS jet forces) F_{aero}.

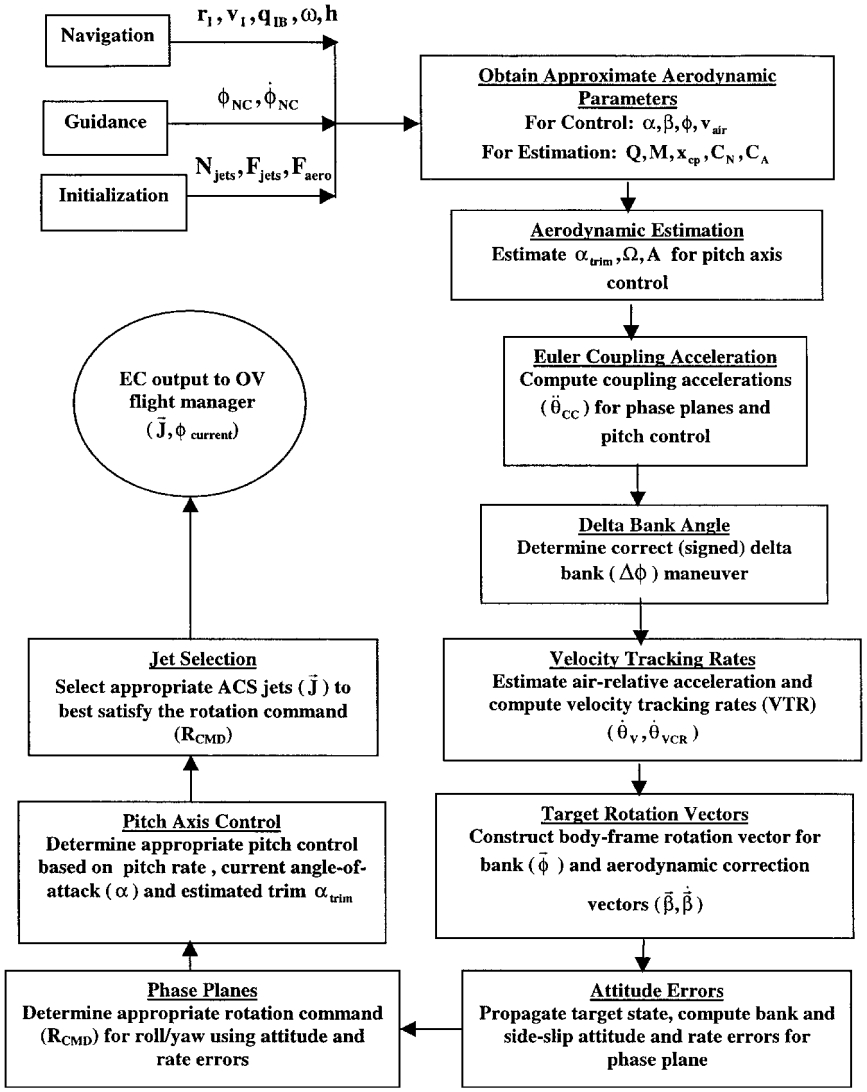

Fig. 2 OV EC logic flow.

The primary responsibility of EC is to execute the just-mentioned bank commands from guidance in an expedient and (fuel) efficient manner, using the information from navigation. The primary EC outputs are the vector of selected ACS jets (a function of the computed R_{CMD}) to bring about the desired control action as well as the current bank angle. The EC controller, then, can be categorized in three main functions: 1) computation of aerodynamic angles and aerodynamic estimation, 2) bank maneuver/side-slip construction and control, and 3) pitch-axis control (angle-of-attack oscillation maintenance). These functions are discussed in the following sections.

Aerodynamic Angles and Estimation

Overview

To perform its various functions, reentry control requires current values of the vehicle angle of attack α, the sideslip angle β, and the bank angle ϕ. To damp the natural oscillation in angle of attack, estimates of the trim angle of attack α_{trim} and estimates of the α oscillation amplitude and frequency are also needed. The design of the reentry controller includes a capability to compute these quantities. Figure 3 shows the architecture of this capability.

Present Values of Aerodynamic Angles

Angle of attack α, side-slip angle β, and total angle of attack α^* are related to v_{air}, the vehicle velocity with respect to the atmosphere expressed in body coordinates, as follows:

$$v_{air} = \|v_{air}\|(\cos\alpha^*, \sin\beta, \sin\alpha) \quad (1)$$

The design uses this relation to obtain α, β, and α^*. A prestored wind profile is used to obtain velocity with respect to the atmosphere from navigated velocity with respect to Earth. The determination of α, β, and α^* thus involves two main sources of error. First, because the embedded GPS/INS (EGI) instruments are misaligned, there will be corresponding errors in the resolution of the velocity vector in the body frame. Second, winds are only crudely modeled. EGI alignment to within ± 1.0 deg is specified. EGI misalignment errors will be essentially constant over the short time (less than 15 min) that reentry control is active.

To estimate the error introduced by mismodeling wind, 400 reentry trajectories were simulated using Gram-95 atmosphere with randomly selected wind parameters. The wind velocity vector was averaged over each simulated trajectory, and the distribution of the average wind vectors was examined. By this method it was found that the average crosswind speed can be expected to be approximately 90 ft/s (1σ). Keeping in mind that the vehicle speed exceeds Mach 10 for almost all of the trajectory, the average angular error that we would incur by neglecting wind will be on the order of arctangent of 0.01, i.e., on the order of 0.5 deg (1σ). Using a wind profile, we hope to incur errors that are smaller than this.

The vehicle bank angle ϕ is, by definition, the angle between the plane spanned by the velocity vector and the inertial position vector (the vertical plane) and the plane spanned by the velocity vector and the vehicle longitudinal x axis. We compute the angle between these planes as the angle between their normal vectors, which are computed as the cross product of the air velocity vector with the navigated position vector and the cross product of the air velocity vector with the vehicle x axis. The dominant source of error in computed ϕ is EGI misalignment.

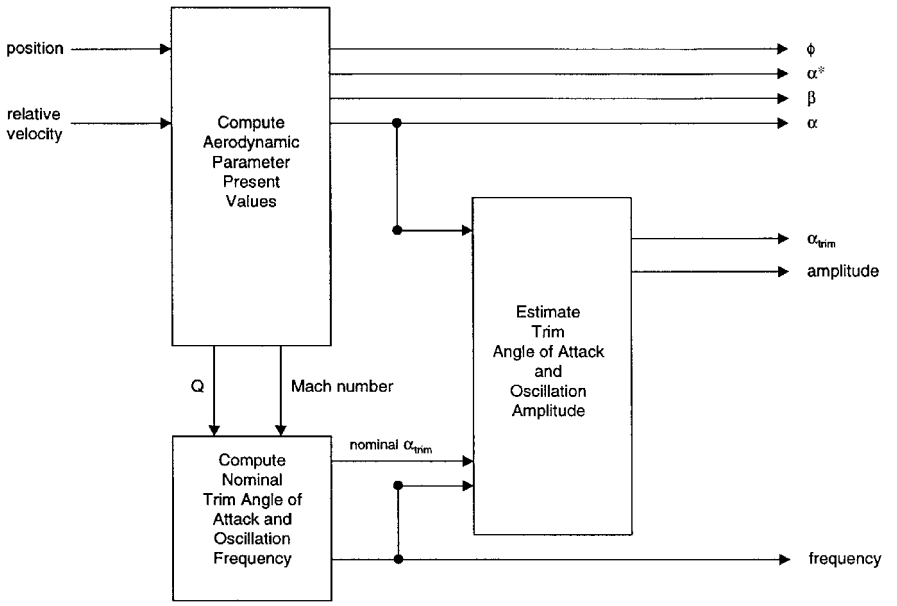

Fig. 3 Aerodynamic parameter estimation.

Present Values of Dynamic Pressure and Mach Number

The design uses prestored tables of atmospheric density ρ and speed of sound v_{sound}; each is parameterized by altitude h. The two tables are provided to the flight system as part of the mission load database. Vehicle altitude is an input to control from the navigation subsystem. Atmospheric density ρ and speed of sound v_{sound} are then found by linear interpolation in the respective tables.

Dynamic pressure Q and Mach number M are computed from ρ, v_{sound}, and $\|v_{\text{air}}\|^2$ in the obvious way:

$$Q = \frac{1}{2}\rho\|v_{\text{air}}\|^2, \qquad M = \frac{\|v_{\text{air}}\|}{v_{\text{sound}}} \tag{2}$$

Error caused by wind mismodeling is insignificant when compared to likely error in predicted atmospheric density.

Mach number is needed only to obtain reference values of vehicle aerodynamic coefficients, as will be discussed presently. Fortunately, the aerodynamic coefficients of the K1 orbital vehicle are very insensitive to errors in Mach number for M greater than 2 (almost all of the controlled reentry because a drogue parachute will be deployed and control will be inactive below Mach 2). Thus a rather large error in computing Mach number is acceptable. Dynamic pressure is used to compute the α oscillation frequency, as will be discussed later. Our design performance is shown to be insensitive to errors in Q of 10–20%.

Nominal Aerodynamic Coefficient Database

Tables of nominal aerodynamic coefficients, parameterized by Mach number M and total angle of attack α^*, are included in the mission-load database. The primary tabulated quantities are the normal and axial aerodynamic force coefficients C_N and C_A and the longitudinal x coordinate of the aerodynamic center of pressure x_{cp}. Initial data for these tables are from wind-tunnel testing. Nominal tables of the partial derivatives with respect to α of these three quantities are included in the database. Partial derivatives are used only in the computation of the α oscillation frequency.

Current values of x_{cp}, C_N, and C_A and of the derivatives $x_{\text{cp},\alpha}$, $C_{N,\alpha}$, and $C_{A,\alpha}$ are computed using two-dimensional linear interpolation in the respective mission-loaded tables. Mach number M and total angle of attack α^* used in this interpolation are the values already computed.

Modeling the Oscillation in Angle of Attack and Estimation of Trim Alpha

To damp the natural oscillation in angle of attack, the controller attempts to null the vehicle pitch rate at the instant when angle of attack is equal to its trim (zero moment) value (see section on Pitch Axis Control). To implement this strategy, the controller requires an estimate of α_{trim}. So as not to use fuel damping, an oscillation whose amplitude is insignificant; an estimate of the oscillation amplitude is also needed.

For each Mach number M the nominal value of trim angle of attack α_{trim} can be obtained by solving for α in the pitch torque balance equation

$$C_N(M, \alpha)[x_{\text{cp}}(M, \alpha) - x_{\text{cg}}] + C_A(M, \alpha)z_{\text{cg}} = 0 \tag{3}$$

Here x_{cg} and z_{cg} denote the position coordinates of the vehicle center of mass. We hold M fixed and vary α, using interpolation in tables of x_{cp}, C_N, and C_A to determine their corresponding values at α.

Although this method allows us to tabulate α_{trim} vs M in advance, there are several reasons that we prefer to estimate α_{trim} in flight for use by control. First, the solution to the torque balance equation is rather sensitive to errors in the aerodynamic coefficients. Values of these coefficients available from wind-tunnel testing can differ significantly from values experienced in flight. Nominal α_{trim} can therefore be seriously in error. Second, the current angle of attack α we compute from vehicle air velocity is incorrect because of EGI misalignment and because of wind errors. If the controller is to act when $\alpha = \alpha_{\text{trim}}$, it would be best if the α_{trim} we compare contained similar errors (i.e., onboard estimation of α_{trim} will serve to compensate the effect of errors in α). Third, knowledge of the α oscillation amplitude is needed by control.

For estimation we model the α oscillation as simple harmonic motion of angular frequency Ω about an equilibrium point. This idea leads to a (slowly time-varying) three-state linear filter. A natural set of state variables is the following: x_1 = equilibrium position (estimated deviation from nominal α_{trim}), x_2 = current displacement from equilibrium (estimated $\alpha - \alpha_{\text{trim}}$), and x_3 = derivative with respect to time of x_2 (scaled to nondimensionalize).

The state dynamics has the form

$$\dot{x} = Ax + bu, \qquad y = c'x \tag{4}$$

where u is external forcing (pitch torque N_{jets} caused by jet firings plus pitch component of the $-\omega \times I\omega$ Euler coupling from the body rate vector ω).

With appropriate scaling of x_3, the 3×3 matrix A is given by

$$A = \begin{bmatrix} 0 & 0 & 0 \\ 0 & 0 & -\Omega \\ 0 & \Omega & 0 \end{bmatrix} \tag{5}$$

and b is of the form

$$b = \begin{bmatrix} 0 \\ 0 \\ b_3 \end{bmatrix} \tag{6}$$

where $b_3 = -1/\Omega I_{YY}$.

The oscillation angular frequency Ω is computed using dynamic pressure Q and nominal aerodynamics coefficients and their derivatives; thus

$$C_{m,\alpha} = C_{N,\alpha}(x_{cp} - x_{cg}) + C_N x_{cp,\alpha} + C_{A,\alpha} z_{cg}, \qquad \Omega^2 = -\frac{QSC_{m,\alpha}}{I_{YY}} \tag{7}$$

The estimator's observable is the difference between the sensed value of α [from Eq. (1)] and the nominal trim value of α (tabulated). With the specified estimator state variables it follows that the observation matrix is given by

$$c' = [1 \quad 1 \quad 0] \tag{8}$$

The state equations for the trim estimator are formed from this model in the usual way:

$$\dot{x} = Ax + bu + L(y - c'x) \tag{9}$$

With this implementation the required estimate of α_{trim} is obtained by adding the state variable x_1 (a correction) to the nominal (tabulated) value of α_{trim}.

The α oscillation amplitude M is readily obtained from the estimator state variables:

$$M^2 = x_2^2 + x_3^2 \tag{10}$$

The 3×1 gain vector L can be chosen using any of various well-known methods. For simplicity and robustness we choose L (which depends on the frequency Ω) using pole placement methods. Because our choice of state variables is nondimensional, it is appropriate to compute gains $L(\Omega)$ for oscillation frequency Ω by rescaling gains for $\Omega = 1$, i.e.,

$$L(\Omega) = \Omega L(1) \tag{11}$$

Viewed as a black-box single-input/single-output system—(observe α, output α_{trim})—the estimator transfer function has the form

$$H(s) = [1 \quad 0 \quad 0] \cdot [s1 - (A - Lc')]^{-1} \cdot L \tag{12}$$

It is useful to consider the Bode plot of the design. The frequency response has the following characteristics: unity gain at $s = 0$ (α_{trim} is found by averaging α) and near zero gain at $s = \pm i\Omega$. (We notch out the anticipated oscillation.) We model the oscillation frequency Ω using nominal, imperfectly known aerodynamic coefficients. To reduce sensitivity to error in nominal Ω, we impose on gain set L the requirement that the estimator gain must be at least -20 dB at frequencies within $\pm 50\%$ of Ω. Figure 4 shows the frequency response of the estimator design (normalized to the case $\Omega = 1$).

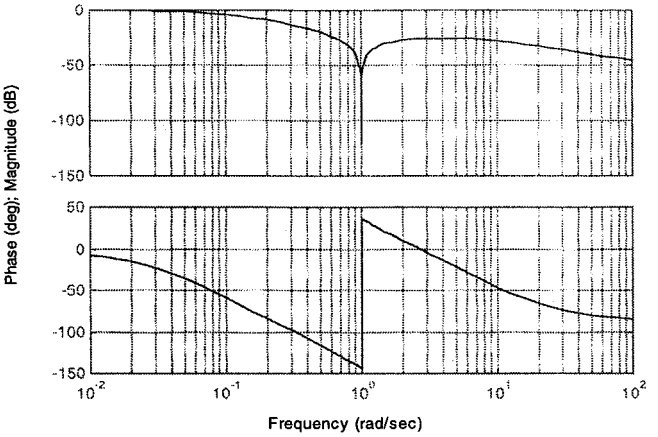

Fig. 4 Estimator frequency response: Bode diagrams.

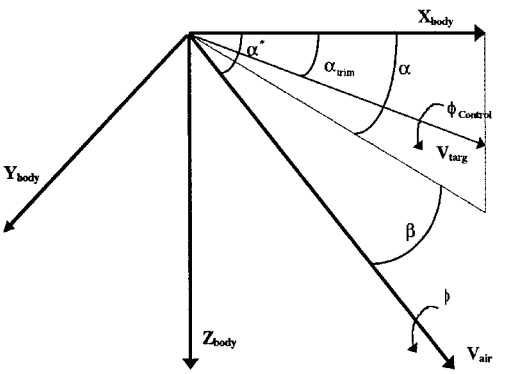

Fig. 5 Aerodynamic angles on the K1 OV.

Aerodynamic Bank Maneuver Control

The primary function of the EC mode is the accurate implementation of the bank angle and bank rate commands from the OV guidance system, received as each guidance cycle (1 Hz). The EC controller operates at 25 Hz. Guidance provides a target bank angle ϕ_{NC} and a signed maneuver rate $\dot{\phi}_{NC}$ to EC. The overall objective is to construct a maneuver profile to accomplish this bank instruction, while simultaneously maintaining the critical aerodynamic conditions, the angle of attack α and the sideslip (β).

Figure 5 depicts the bank angle as well as the angle of attack and sideslip as defined in the K1 OV body-fixed reference frame. The actual angle of attack and the sideslip are measured with respect to the wind relative velocity direction v_{air}. The total angle of attack (α^*), which is the angle between the vehicle x (roll) axis and the v_{air}, is also depicted in Fig. 5. The target aerodynamic configuration of the vehicle is such that the angle of attack and sideslip are at the trim point (α_{trim} and β_{trim}). Note that α_{trim} is generated by the EC estimator, and β_{trim} is assumed equal to 0. Hence, the target velocity vector v_{targ}, is defined as the zero sideslip velocity, the relative velocity that would result if the angle of attack were precisely at α_{trim} and the sideslip were exactly zero. The normalized version of this target velocity, expressed in the body frame, is computed as

$$\hat{v}_{targ} = [\cos(\alpha_{trim}), 0, \sin(\alpha_{trim})] \tag{13}$$

and is used by the EC system as the desired rotation axis for the bank maneuvers. Hence,

$$\hat{u}_\phi = \hat{v}_{targ} \tag{14}$$

The control system constructs bank maneuvers by applying the commanded delta-bank angle about the bank rotation axis $\hat{u}_\phi$.

Determination of Signed Delta-Bank Angle

The determination of the correct signed delta-bank angle is a critical component of the entry controller's ability to achieve the desired effect on the vehicle's return trajectory. The algorithm must correctly evaluate not only the target bank angle but also the target maneuver direction. Because the guidance bank and bank rate commands are based only on the preceding and current bank angle commands and because it is, in general, unrealistic to presume that the controller will exactly attain the desired bank angles, there is a risk of EC misinterpreting the intended direction for the maneuver. Such a scenario is depicted in Fig. 6. Suppose the commanded and actual bank state are as shown in the figure. Guidance provides a desired bank rate based on the current and earlier bank angle commands.

Hence, if the guidance objective is simply to go from ϕ_{OC} to ϕ_{NC} the short way, then the sign of the $\dot{\phi}_{NC}$ will be positive. Given the location of the actual bank angle $\phi_{current}$, however, this commanded

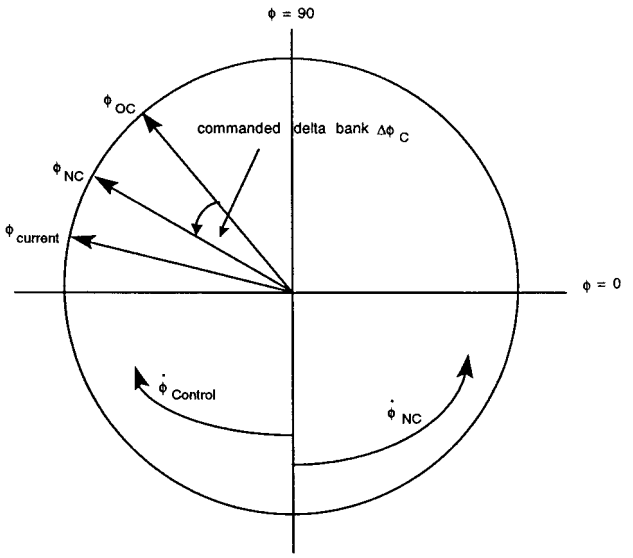

Fig. 6 Bank angle direction ambiguity.

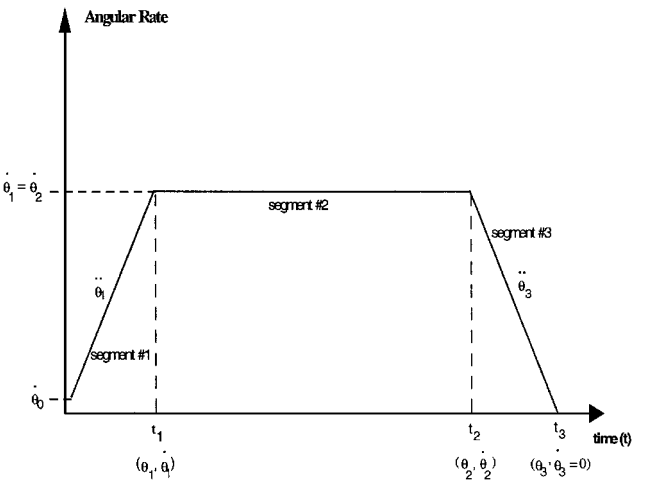

Fig. 7 Maneuver control segments.

rate would result in the controller constructing a very large bank maneuver. The integrated effect of such an erroneous maneuver, in terms of the time profile of the vehicle lift vector, must be avoided. Hence, under certain conditions the controller must be intelligent enough to defy the direction commanded by the guidance bank maneuver rate and ascertain what the true objective of the current commands are, based on the current and earlier commands as well as the actual bank angle.

Computation of Target Rotation Vectors

Once the correct delta-bank $\Delta\phi$ angle is computed, the current rotation vector for the desired bank maneuver may be constructed. As just described, the rotation axis for the bank maneuver is given by Eq. (14). Therefore, the rotation vector for the bank is simply

$$\boldsymbol{\phi} = \Delta\phi\hat{u}_{\phi} \tag{15}$$

This will produce roll and yaw maneuvers only because, as shown in Fig. 5, the target bank maneuver is about an axis in the body x–z plane. The current vehicle sideslip β is computed in the aerodynamic angle computations within EC. The desired sideslip is $\beta_{\text{trim}} = 0$. There are several reasons for this trim value. First, the baseline configuration for the K1 OV provides a center-of-mass (COM) offset, which is along only the body z axis. (This offset is largely responsible for the OV having a nonzero trim angle of attack, resulting in controllability.) Because the vehicle stability characteristics are such that the COM tends to remain on the side of the vehicle facing the relative velocity vector, it would be inefficient from a fuel perspective to attempt to hold a different β_{trim}. Additionally, the K1 OV is thermally enhanced on the side of the vehicle corresponding to $\beta = 0$. Holding a different side of the vehicle into the wind would risk damage from heat exposure.

To control the sideslip condition in EC, it is shown in Fig. 5 that β, like ϕ, is a roll/yaw rotation. Corrections to account for a nonzero sideslip error, described in Ref. 1, are computed as follows:

$$\boldsymbol{\beta} = \beta K_{\beta}[-\sin(\alpha), 0, \cos(\alpha)], \qquad \dot{\boldsymbol{\beta}} = \dot{\beta} K_{\beta}[-\sin(\alpha), 0, \cos(\alpha)] \tag{16}$$

Note, the actual (measured) angle of attack is used in these computations. Equations (15) and (16) provide the extent of the attitude corrections required for roll and yaw maneuvers. The sideslip corrections, given by Eq. (16), are complete in that they are provided in this form to the calculation of total roll/yaw attitude and rate errors (a sum of sideslip and bank errors) for the phase-plane logic. The bank vector given by Eq. (15), however, is most efficiently executed by first resolving the total maneuver into individual segments.

Construction of Bank Maneuver Segments

If the total angular error associated with the target bank angle is greater than a database threshold, a bank maneuver will be constructed that results in the classic three-segment ramp-up, coast, ramp-down sequence. Figure 7 depicts a typical maneuver structure, listing the critical angles and rates associated with each segment.

The commanded bank angle and rate from guidance are first validated to ensure that the rate is achievable for the proposed angular changes in roll and yaw. The minimum required travel for the commanded rate is given by

$$\Delta\theta_{\text{req}} = \left| \frac{\dot{\theta}^2_{\text{coast}}}{\ddot{\theta}_{\text{man}}} \right| \tag{17}$$

where the $\ddot{\theta}_{\text{man}}$ is the nominal expected acceleration capability from the jets. If the desired $\Delta\theta$ is smaller than this minimum, a new maneuver rate is computed as

$$\dot{\theta}_{\text{coast}} = \left\{ \left| \frac{(\Delta\theta)(\ddot{\theta}_{\text{man}})}{(1 + K_{\dot{\theta}})} \right| \right\}^{\frac{1}{2}} \tag{18}$$

Note that this logic is applied both to the roll portion and to the yaw portion of the maneuver. The rotation vector of Eq. (15) is simply resolved into roll and yaw parts, and the axes are processed individually. Here $K_{\dot{\theta}}$ is a database gain that represents the ratio of coast (segment 2) duration (Δt_2) to acceleration (segment 1) duration (Δt_1). Then, nominal maneuver segments can be constructed using the adjusted maneuver rate, just shown, the nominal control acceleration, and the desired angular change. For example, the nominal first (acceleration) segment of the maneuver is described in Eq. (19) using a simple quadratic model. Here, θ_1 is the total angle change from maneuver start to t_1 at the end of segment 1. Also, $\dot{\theta}_1$ is the rate at the end of segment 1, and $\ddot{\theta}_1$ is the acceleration during segment 1. The initial angular rate is given by $\dot{\theta}_0$:

$$\dot{\theta}_1 = |\dot{\theta}_{\text{coast}}|\,\text{sign}(\Delta\theta), \qquad \ddot{\theta}_1 = |\ddot{\theta}_{\text{man}}|\,\text{sign}(\dot{\theta}_1 - \dot{\theta}_0)$$
$$\Delta t_1 = |(\dot{\theta}_1 - \dot{\theta}_0)/\ddot{\theta}_1|, \qquad \theta_1 = \dot{\theta}_0 \Delta t_1 + \tfrac{1}{2}\ddot{\theta}_1 \Delta t_1^2 \tag{19}$$

Similar computations can be accomplished for the coast segment (2) and the deceleration segment (3).

Using the anticipated durations for the three segments in both roll and yaw, computed as in Eq. (19), the coast rates and acceleration magnitudes are adjusted again so that a maneuver coordinated in roll and yaw is designed. This is accomplished by ensuring that the start and end times of each of the maneuver segments are the same for both axes. This feature is necessary to minimize the perturbations to the trim condition, which result from performing a bank maneuver. In particular, an uncoordinated bank would result in a temporary increase in the sideslip error. The resulting coast segment rates

$\dot{\theta}_1$ and segment 1 and 3 acceleration values $\ddot{\theta}_1$ and $\ddot{\theta}_3$ are now used to propagate the target attitudes and rates for the maneuver.

Computation of Velocity Tracking Rates

The velocity tracking rate (VTR) routine computes the effective angular rate of the bank vector $\dot{\theta}_{\mathrm{VCR}}$ and the angular rate of the air-relative velocity vector $\dot{\theta}_V$. These vectors are computed in the inertial frame and then transformed to the body-fixed frame. The resulting rotational rate vectors are then used in the maneuver design and phase-plane error computations to cause the vehicle to track the inertial motions of the bank and velocity vectors. This approach provides improved controller performance during flight phases where vehicle accelerations are high, rendering the nominal bank maneuver design approach insufficient for tracking the required state. The velocity vector rate is simply the angular motion of the velocity vector, resulting from inertial forces acting on the velocity vector, as seen in the vehicle frame. The bank vector rate is the angular motion of the vector formed by the cross product of inertial velocity and position (i.e., the bank vector), resulting from inertial forces acting on this vector, as seen in the vehicle frame. As this vector is exposed to inertial forces on the vehicle, the resulting motions cause undesired bank angle rates.

The procedure is to compute the tangential portion of the acceleration vector that directly influences the effective rotational rate of the air-relative velocity vector. Similarly, we compute the tangential component of the vector representing the time rate of change of the bank vector vcr_I. In this way, we attempt to account proactively for rates of the aerodynamic angles caused by inertial accelerations on the vehicle.

First, compute the cross product of velocity and acceleration in the inertial frame and its magnitude:

$$v_{\mathrm{mag}} = \|v_I\|_2, \qquad vca_I = v_I \times a_I, \qquad vca_{\mathrm{mag}} = \|vca_I\|_2 \tag{20}$$

Now, compute the tangential portion of the acceleration vector and its magnitude:

$$a_{I\_t} = vca_I / v_{\mathrm{mag}}, \qquad a_{t\_\mathrm{mag}} = \|a_{I\_t}\|_2 \tag{21}$$

The bank vector in inertial space vcr_I and its time derivative are given by

$$vcr_I = v_I \times r_I, \qquad vcr_{\mathrm{mag}} = \|vcr_I\|_2$$

$$acr_I = \frac{\mathrm{d}}{\mathrm{d}t}(vcr_I) = a_I \times r_I \tag{22}$$

The tangential portion of the acr vector and its magnitude is

$$vcrcacr_I = vcr_I \times acr_I, \qquad vcrcacr_{\mathrm{mag}} = \|vcrcacr_I\|_2$$

$$acr_{I\_t} = \frac{vcrcacr_I}{vcr_{\mathrm{mag}}}, \qquad acr_{t\_\mathrm{mag}} = \|acr_{I\_t}\|_2 \tag{23}$$

Using the components of the time derivatives tangential to the velocity and bank vectors, we can write the effective angular rates of the velocity and bank vectors and construct the corresponding rate vectors in inertial and then body frame.

Here the magnitude of the velocity vector rate and the bank vector rate is

$$\dot{\theta}_{V\_\mathrm{mag}} = \frac{a_{t\_\mathrm{mag}}}{V_{\mathrm{mag}}}, \qquad \dot{\theta}_{\mathrm{VCR}\_\mathrm{mag}} = \frac{acr_{t\_\mathrm{mag}}}{vcr_{\mathrm{mag}}} \tag{24}$$

Constructing the corresponding rate vectors in the inertial frame,

$$\dot{\theta}_{V\_I} = \dot{\theta}_{V\_\mathrm{mag}}\left(\frac{vca_I}{vca_{\mathrm{mag}}}\right), \qquad \dot{\theta}_{\mathrm{VCR}\_I} = \dot{\theta}_{\mathrm{VCR}\_\mathrm{mag}}\left(\frac{vcrcacr_I}{vcrcacr_{\mathrm{mag}}}\right) \tag{25}$$

Finally, transform the velocity and bank rate vectors from the inertial frame to the body frame so that they may be incorporated into the controller phase-plane rate error computations. Here, ${}_B T_I$ represents the direction cosine matrix that transforms a vector expressed in inertial space to the equivalent one expressed in body-fixed space:

$$\dot{\theta}_V = \dot{\theta}_{V\_B} = [{}_B T_I][\dot{\theta}_{V\_I}], \qquad \dot{\theta}_{\mathrm{VCR}} = \dot{\theta}_{\mathrm{VCR}\_B} = [{}_B T_I][\dot{\theta}_{\mathrm{VCR}\_I}] \tag{26}$$

Computation of Angle and Rate Errors

The angle and rate errors associated with the bank maneuvers as well as the sideslip maintenance are computed by simply differencing the target angles and rates and the actual angles and rates. In the case of the bank maneuvers, the target angles represent the amount of rotation remaining in the current maneuver. This is quantified by propagating a target rotation angle θ_d representing the desired amount of remaining rotation (in the particular axis) at the current time into the maneuver t_{man}, using the nominal control acceleration $\ddot{\theta}_{\mathrm{man}}$ and any initial rate ω_{old}. Similarly, the target angular rate $\dot{\theta}_d$ is propagated using the $\ddot{\theta}_{\mathrm{man}}$ and t_{man}. Once the current maneuver segment is identified, the target angles and rates may be computed. The segment 1 targets are

$$\theta_d(i) = \boldsymbol{\theta}_{\mathrm{old}}(i) - t_{\mathrm{man}}(i)[\omega_{\mathrm{old}}(i)] - t^2_{\mathrm{man}}(i)\left[\tfrac{1}{2}\ddot{\theta}_1(i)\right]$$

$$\dot{\theta}_d(i) = \omega_{\mathrm{old}}(i) + t_{\mathrm{man}}(i)[\ddot{\theta}_1(i)] \tag{27}$$

A similar calculation is done for segment 2 (coast) in Eq. (28). The bank rate component $\dot{\theta}_{\mathrm{VCR}}$ is included in the target rates for this segment as it is desired that the commanded rate for the maneuver be supplemented by the residual rate of the bank vector. In other words, it is desired that the vehicle always track the $\dot{\theta}_{\mathrm{VCR}}$ rate, whether in a maneuver or not. If in a maneuver, this rate is in addition to the target maneuver rate. It is not included in the target angle profile, however, because the actual rotation rate of the bank vector should completely compensate for the rate supplement resulting in 0 net angular effect on the rotation vector:

$$\theta_d(i) = \theta_1(i) - \lfloor \dot{\theta}_2(i) \rfloor [t_{\mathrm{man}}(i) - t_1(i)]$$

$$\dot{\theta}_d(i) = [\dot{\theta}_2(i)] + \dot{\theta}_{\mathrm{VCR}}(i) \tag{28}$$

The segment 3 targets are similar and include the $\dot{\theta}_{\mathrm{VCR}}$ rates as well.

Once the segment number and target angles and rates are known, the errors may be calculated. The angle errors are computed as follows:

$$\theta'_\varepsilon(i) = \theta_d(i) - \boldsymbol{\theta}(i), \qquad \theta_\varepsilon(i) = K_\phi(i)\{W_\theta(i)[\theta'_\varepsilon(i)]\} - \boldsymbol{\beta}(i) \tag{29}$$

and the rate errors are computed as

$$\dot{\theta}_\varepsilon(i) = K_\phi(i)[\omega(i) - \dot{\theta}_d(i)] - \dot{\boldsymbol{\beta}}(i) - \dot{\theta}_V(i) \tag{30}$$

The angle errors are computed as the difference between the desired amount of remaining rotation for a particular point in the maneuver θ_d less the actual amount of rotation remaining for that point in the maneuver $\boldsymbol{\theta}$ supplemented with appropriate sideslip errors $\boldsymbol{\beta}$. The rate error is computed as the difference between the actual rate and the target rate $\dot{\theta}_d$ supplemented with the corresponding sideslip error rates $\dot{\boldsymbol{\beta}}$. Additionally, the rate of the velocity vector $\dot{\theta}_V$ is incorporated into the overall rate error to aid in anticipating sideslip motion. The gains K_ϕ and $K_{\dot{\phi}}$ and the weighting factor W_θ are used to prioritize the individual components of the errors.

Phase-Plane Processing

The attitude and rate errors are computed using the preceding methods and are then sent to the phase-plane logic to generate the appropriate rotation command vector R_{CMD}. The detailed processing of the phase-plane logic employed in the K1 system can be found in Ref. 2. A similar implementation, used for the Apollo Program, is described in Ref. 3. Additional theoretical background is provided in Refs. 4 and 5. Figure 8 depicts the basic structure of the upper half of the phase plane.

The x axis of the phase plane is the attitude angle error, and the y axis is the attitude rate error. The S1, S2, S3, S4, and S5 are switch curves that dictate the control action. The S1 and S2 curves are derived from optimal control theory as discussed in Ref. 4

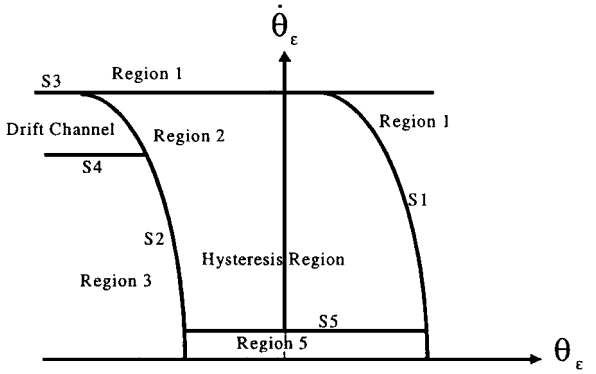

Fig. 8 Basic phase-plane structure (upper half).

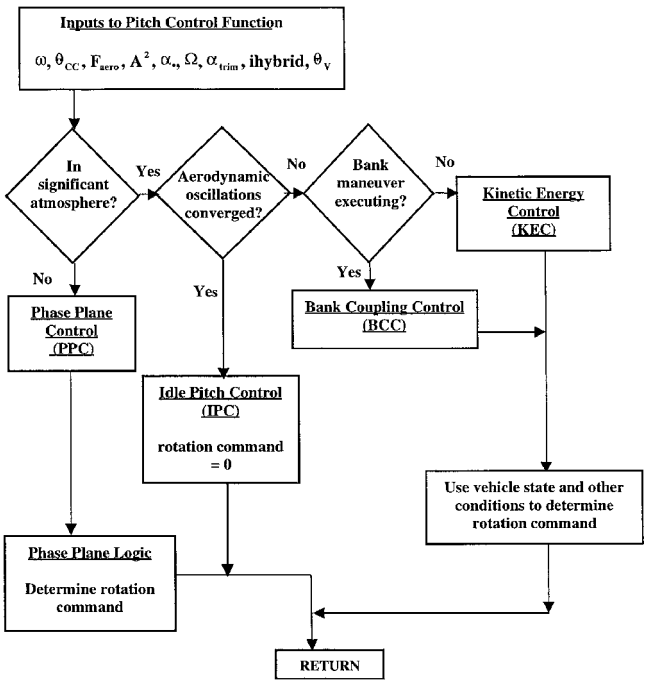

Fig. 9 Pitch control high-level logic flow.

supplemented with attitude deadbands. They are a function of the estimated control acceleration capability for the particular axis. The S3 curve represents the rate error limits, and the S4 curve defines the drift channel. The drift channel, as well as S5 defining region 5, is used to minimize propellant usage. No firings occur while in region 5 or in the drift channel. Generally, appropriate jet firings will occur while the phase point is in regions 1 and 3, and firings can occur while in region 2. The primary objective is to drive the rate errors $\dot{\theta}_\varepsilon$ in a direction of opposite polarity of the angle errors θ_ε. The magnitude of the target rate error depends on the magnitude of the angle error. The lower half of the phase plane is essentially the mirror image of the upper half, offset along the x axis to allow access to region 5 from outside the hysteresis region. The output of the phase plane is the rotation command vector R_{CMD}, which describes the polarity (+1, −1, or 0) of the required angular impulse.

Pitch-Axis Control

The nature of the entry aerodynamics is such that control of the pitch axis requires different considerations than those of the roll and yaw axes. The pitch control routine is responsible for control decisions for the vehicle pitch axis only. The module generates near optimal pitch-axis commands intended to dissipate undesired kinetic energy. The objective is to minimize angle-of-attack α deviations from the trim condition α_{trim} while tracking the vehicle's trajectory curvature. Depending on current flight conditions, the algorithm takes one of four different approaches, as shown in Fig. 9. The four different control strategies are 1) phase-plane control (PPC), 2) bank coupling control, 3) kinetic energy control (KEC), and 4) idle pitch control (IPC).

The first step in the routine is to determine if PPC is appropriate. In the early stages of reentry, the pitch rate and attitude may be controlled by simple phase planes, as described in the preceding section. PPC is used whenever the aerodynamic axial force $F_{\mathrm{AERO\_}X}$ is determined to be less than a predetermined threshold F_{ENTRY}. A low aerodynamic axial force indicates that the current aerodynamic forces do not have a significant effect on the dynamics of the vehicle, thereby allowing the vehicle sufficient control authority to attain an arbitrary pitch rate or angle. The desired attitude is the current α_{trim}, and the desired rate is that necessary to maintain the trajectory curvature. Hence, the attitude and rate errors for the phase planes are computed as

$$\theta_e = (\alpha - \alpha_{\mathrm{trim}}), \qquad \dot{\theta}_e = \omega_y - \dot{\theta}_{V\_y} \tag{31}$$

Note the inclusion of the $\dot{\theta}_V$ (y axis) term, from the VTR computation, to track the rotating velocity vector. In Eq. (31) ω_y is the current actual pitch rate. If it has been determined that the vehicle is currently in a regime of significant aerodynamic axial force, the next check is to evaluate if the aerodynamic oscillations have attained the converged condition. If they have converged, then no pitch-axis control action is taken ($R_{\mathrm{CMD\_}y} = 0$); also, status is set to IPC. Otherwise, the algorithm must determine the particular control phase necessary to best damp the pitch-axis rotational kinetic energy of the system.

If the vehicle is in significant atmosphere but the oscillations have not converged, the algorithm determines if a coordinated bank maneuver is currently being accomplished. When the vehicle enters a coordinated bank, Euler coupling effects from the roll and yaw axes can have a significant effect on the angle-of-attack motion. To prevent these coupling effects from accumulating, the algorithm applies a simple approach to offsetting the kinetic energy imparted on the pitch axis by this cross coupling. The coupling results in a pitch acceleration that could increase the angle of attack and excite a larger aerodynamic oscillation. This effect is countered by first integrating the estimated energy transferred into pitch by the Euler coupling:

$$\Delta E_{CC} = \int \ddot{\theta}_{CC} I_{YY} \omega_Y \, \mathrm{d}t \tag{32}$$

where the coupling acceleration is

$$\ddot{\theta}_{CC} = -\frac{1}{I_{YY}} \left[\begin{array}{c} -I_{YZ}\omega_X\omega_Y + I_{YY}\omega_Y\omega_Z + (I_{XX} - I_{ZZ})\omega_X\omega_Z \\ +I_{XZ}\left(\omega_Z^2 - \omega_X^2\right) \end{array} \right] \tag{33}$$

This is then compared with the amount of energy that could potentially be removed by a control firing:

$$\Delta E_C = \ddot{\theta}_C I_{YY} \omega_Y \Delta t_p \tag{34}$$

In the preceding equations I_{YY} is the (2,2) component of the inertia tensor; ω_X, ω_Y, ω_Z, are the current roll, pitch, and yaw body rates; and $\ddot{\theta}_C$ is the nominal expected control acceleration, in this case for the pitch axis. When the accumulated energy change from Eq. (32) exceeds that from Eq. (34), a jet firing is commanded, which opposes the existing pitch rate. In this manner the effects of Euler coupling on the angle-of-attack oscillation are essentially canceled.

Simulation Results

The attitude control system design described in the preceding text was implemented in a high-fidelity simulation, the K1 Integrated Vehicle Simulation, at Draper Laboratory. The simulation uses aerodynamic models and vehicle configuration characteristics obtained from Kistler Aerospace. The results presented here are from a nominal simulation run. In particular, the environment included no unknown wind conditions, resulting in perfect knowledge of the air-relative velocity vector, perfectly known mass properties

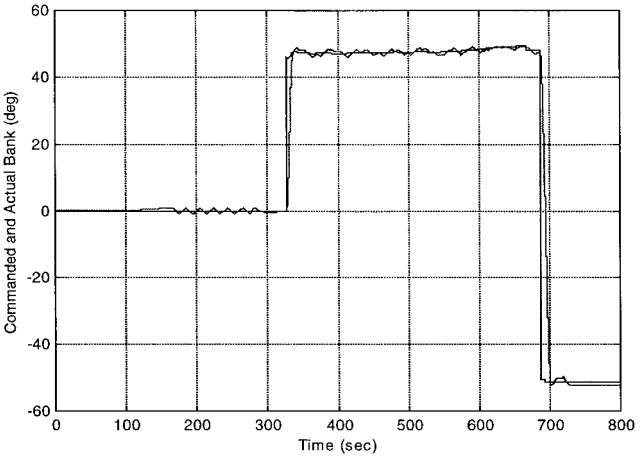

Fig. 10 Commanded bank and actual bank.

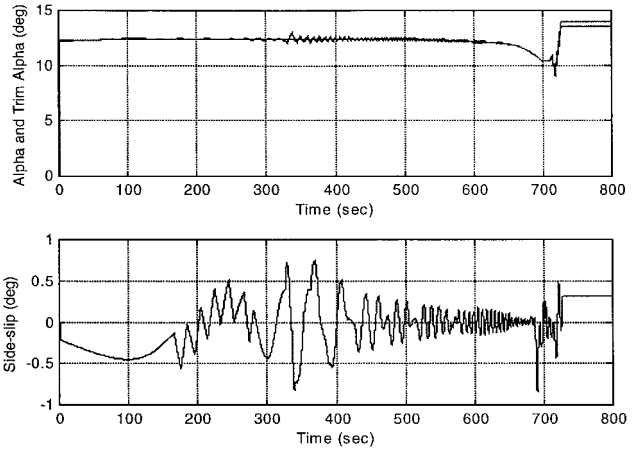

Fig. 12 Trim and actual angle of attack and sideslip.

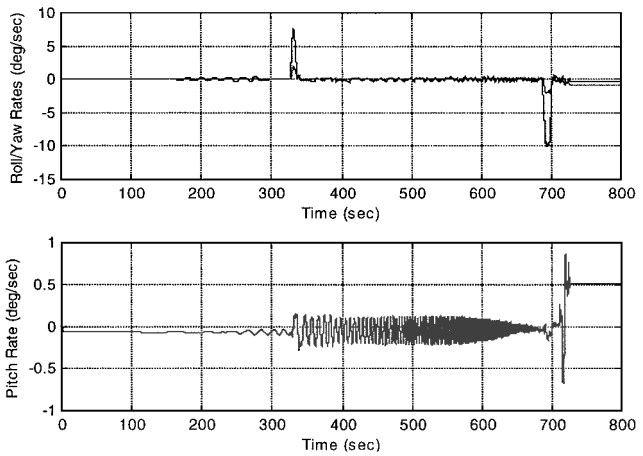

Fig. 11 Vehicle angular body rates.

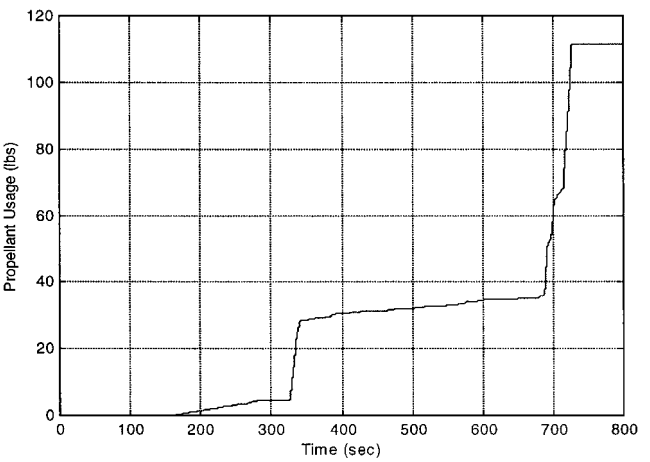

Fig. 13 Propellant usage.

and a perfect aerodynamics model. That is, the flight software models matched the simulation environment for these parameters. Interestingly, the control system is somewhat insensitive to aerodynamic related errors, including modeling errors and measurement errors primarily because of the manner in which the aerodynamic conditions are controlled. Errors in the mass properties of the vehicle will result in added propellant consumption but are not included here.

Figure 10 shows the commanded bank angle ϕ_{NC} vs actual (idealized) bank angle $\phi_{current}$. The commanded angle is generated by the OV guidance and is represented by the straight, steady lines in the plot. The actual bank plot generally oscillates about the commanded angle, primarily because of limit cycling in the phase plane. Some of this chatter can be eliminated by further refinement of the gains and phase-plane limit parameters, although limitations resulting from jet modeling errors and minimum impulse bits dictate that some deadbanding will persist. The actual bank tracks the command to within the 1-deg deadband, which results in the vehicle hitting the target landing zone. Figure 11 shows the vehicle angular rate profiles. The top plot in Fig. 11 is the roll/yaw rate plots. These are overplotted to highlight the nature of the coordinated bank maneuver accomplished. The roll rates attain the noticeably higher rates during the large maneuvers, approximately 7 and 10 deg/s, respectively, whereas the yaw rates, seen inside the roll profiles, attain roughly 2 deg/s only. This result is because at a trim angle of attack of roughly 11 deg the bank rotation axis is predominantly roll. Also, from these plots it is clear that nearly coordinated maneuvers are accomplished. The bottom plot of Fig. 11 shows the pitch-axis rates. The top plot of Fig. 12 is the actual angle of attack α overplotted with the estimated trim angle of attack α_{trim}. During nominal pitch control operation (KEC), the jets will fire only when α is near α_{trim}, and the pitch rate (Fig. 11) exceeds a specified limit (0.2 deg/s). Hence, in this scenario, very little pitch control is required during much of the run. The bottom plot of Fig. 12 is the actual sideslip β angle. The sideslip is controlled to within the 1-deg deadband, with the only substantial disturbances occurring during the large bank maneuvers (about 300 s and again near 700 s). This is primarily because of Euler coupling effects into the yaw axis. Finally, the total propellant usage is shown in Fig. 13. The substantial jumps in fuel occur also during the two large bank maneuvers. Smaller increases are attributable to phase-plane limit cycling and any pitch and sideslip control actions that have occurred.

Conclusions

The design of a system that can successfully control the Kistler K1 Orbital Vehicle from shortly after the completion of a deorbit burn through atmospheric reentry and until stabilization parachute deployment has been described. This flight phase lasts less than 15 min, but flight conditions change drastically in this period: altitude goes from greater than 400,000 ft to less than 100,000 ft; Mach number reaches a maximum of greater than 25 and then diminishes until it is less than 2.6; dynamic pressure attains a maximum value greater than 1000 lb/ft^2. Vehicle angle of attack is controlled to within a fraction of a degree of its trim value for the majority of the reentry trajectory. The vehicle travels more than 4000 miles, while achieving a position error at stabilization parachute deployment typically under 5000 ft. This is largely because of jet commands that control the bank-about-velocity maneuvers and maintain the aerodynamic conditions. This performance is achieved using typically less than 150 lb of propellant.

Acknowledgments

This work was done at the Charles Stark Draper Laboratory under Contract 191-4000, supported by the Kistler Aerospace

Corporation. The contents and ideas presented in this work do not necessarily reflect those of the Kistler Aerospace Corporation. The authors also wish to thank Draper Laboratory staff members Michael Ricard and Barry Fink and Draper Laboratory Fellow Robert Bibeau for their technical support and contributions that made this work possible.

References

[1]"Aeroassist Flight Experiment," McDonnell Douglas Space Systems Co., Attitude Control System Design Book MDC91W5015, Huntsville, AL, June 1991, pp. 6-245–6-250.

[2]*Software Requirements Specification for the Flight Manager CSCI of the K-1 Orbital Vehicle*, Charles Stark Draper Lab., Cambridge, MA, May 1998.

[3]"Apollo Guidance, Navigation and Control," Massachusetts Inst. of Technology and Charles Stark Draper Lab., Technical Software Rept. R-700, Cambridge, MA, July 1971, pp. 220–230.

[4]Ho, Y., and Bryson, A. E., *Applied Optimal Control*, Hemisphere, New York, 1975, pp. 110–120.

[5]Junkins, J. L., and Turner, J. D., *Optimal Spacecraft Rotational Maneuvers*, Elsevier, New York, 1986, pp. 195–200.

F. H. Lutze Jr.
Associate Editor